2021 43rd Annual International Conference of the
IEEE Engineering in Medicine & Biology Society (EMBC)
Oct 31 - Nov 4, 2021. Virtual Conference

2021 43rd Annual International Conference of the IEEE Engineering in Medicine & Biology Society (EMBC) | 978-1-7281-1179-7/21/$31.00 ©2021 IEEE | DOI: 10.1109/EMBC46164.2021.9630889

Design of Novel End-effectors for Robot-assisted Swab Sampling to Combat Respiratory Infectious Diseases

Ruijie Tang, Jia Zheng, Shuangyi Wang

***Abstract*—The COVID-19 outbreak has caused the mortality worldwide and the use of swab sampling is a common way of screening and diagnosis. To combat respiratory infectious diseases and assist sampling, robots have been utilized and shown promising potentials. Nonetheless, a safe, patient-friendly, and low-cost swabbing system would be crucial for the practical implementation of robots in hospitals or inspection stations. In this study, we proposed two recyclable and cost-efficient end-effector designs that can be equipped at the distal end of a robot to passively regulate or actively sense the force exerted onto patients. One way is to introduce passive compliant mechanisms with soft material to increase the flexibility of the swabbing system, while the other way is utilizing a force-sensing gripper with embedded optoelectronic sensors to actively sense the force or torque. The proposed designs were modelled computationally and tested experimentally. It is identified that the passive compliant mechanisms can increase the flexibility of the swabbing system when subjected to the lateral force and mitigate the vertical force resulted from buckling. The lateral force range that the force-sensing gripper can detect is 0-0.35 N and the vertical force range causing buckling effect that can be sensed by gripper is 1.5-2.5 N.**

I. Introduction

The COVID-19 has spread rapidly and caused immeasurable losses to the world. To control the spread, oropharyngeal (OP) or nasopharyngeal (NP) swab samplings are common approaches of collecting the specimens for screening and diagnosis. Performing such procedures requires medical staffs to be in close contacts with patients, which leaves them susceptible to the infection of the disease through respiratory droplets and contact transmissions. In view of such challenges, teleoperated and autonomous robots have shown promising potentials in reducing the cross-infection risk. This has been thoroughly reviewed in [1-3]. With the use of robots, the components that come in close contacts with patients can be readily replaced and more thoroughly disinfected. Several sampling robots were therefore designed, fabricated and tested, such as the systems reported in [4-7]. As expected clinically, a safe and smooth swabbing process is necessary when the robots are used for such procedures.

To date, several studies have investigated possible measures that provide safe, and stable sampling experience. In [5], a commercial force sensor was integrated into the end-effector for safety regulation. In [6], an elastomer micro-pneumatic actuator (MPA) was used to adjust the offset distance of swab and offers compliance to reduce shocks caused by contacts between swab and oral cavity. In [7], force was generated by a soft robotic swab consisting of origami-based segment. The soft bending actuator was proved to be similar to a professional medical staff. In [8], a visual system was added onto a UR5 arm to monitor the sampling task. Nonetheless, the above safety measures would encounter some challenges when coming to massive use, e.g., the commercial force sensor and visual camera can increase the cost of the system and the MPA requires molding process and increases difficulties in integration.

In this study, we proposed two detachable, recyclable, and cost-efficient end-effectors that can be equipped at the distal end of a robot to passively regulate or actively sense the force exerted onto patients (Fig. 1): (1) passive compliant mechanisms with soft materials to increase the flexibility of the swabbing system, so as to decrease the force that acts upon the patient; (2) an active force-sensing gripper with embedded optoelectronic sensors to detect the force, which can be used as feedback to guide the robot to adjust its posture based on various control strategies, e.g., the impedance control reported in [9]. Both the above designs could be detached after the swabbing to be disinfected, then recycled.

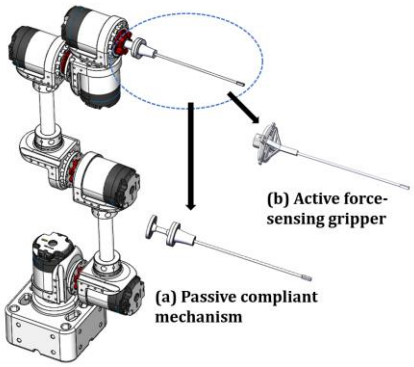

Fig. 1. Conceptual illustration of the proposed two end-effector designs: (a) passive compliant mechanism and (b) active force-sensing gripper.

II. Design and Working Principle

A. Passive Compliant Mechanisms

The design consists of a fixture to hold the swab in place and a passive mechanism with different configurations to introduce extra compliance (Fig. 2). The base of the compliant mechanism is mounted to a connector, which can be further attached to a robot. The compliant mechanism was 3D printed using Thermoplastic polyurethane (TPU), with a Young's Modulus of 8 MPa and a Poisson's ratio of 0.45.

This work was supported in part by the Chinese Academy of Sciences, Institute of Automation and in part by the National Natural Science Foundation of China (62003339). *(Ruijie Tang and Jia Zheng are co-first authors.) (Corresponding author: Shuangyi Wang)*.

R. Tang and S. Wang are with the State Key Laboratory of Management and Control for Complex Systems, Institute of Automation, Chinese Academy of Sciences, Beijing 100190, China (e-mail: ruijie.tang@ia.ac.cn, shuangyi.wang@ia.ac.cn).

J. Zheng is with the School of General Engineering, Beihang University, China (zhengjia210@buaa.edu.cn).

When the tip of the swab touches upon the nasal or the oral cavity, there will be force acting upon the swab and as a result the swab will bend. Because of the soft structure is made of TPU that has a Young's Modulus smaller than the material of the swab stick, additional compliance is introduced with bending motions generated by the mechanism through body deformation to adaptively adjust the posture of the swab, avoiding excessive force due to the bending of the swab stick.

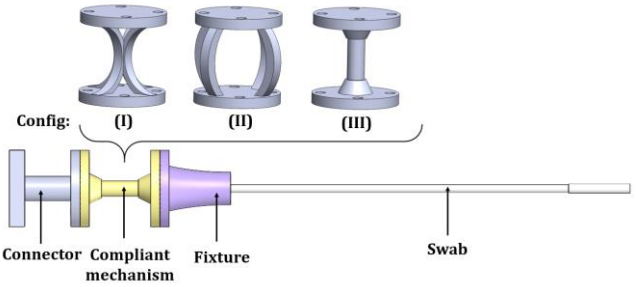

Fig. 2. Schematic illustration of the end-effector with passive compliant mechanisms. Three different options were investigated.

B. Active Force-sensing Gripper

The design contains a bottom board, four optoelectronic sensors (QRE1113, Fair child Semiconductor, California, the United States), a connector, and a gripper to hold the swab (Fig. 3). Because of the compliance of the selected material, force and torque at the tip of the swab can cause the deflections of the beam segments of the gripper, which can be detected by the embedded reflective-based optoelectronic sensors (characteristic curve shown in Fig. 3). The initial gap between the sensors and the deflected segments was set within 0.8 mm to ensure the perceptive working range is highly linear. In this work, Acrylonitrile Butadiene Styrene (ABS) was selected as the 3D-printing material of the gripper, while the bottom board was 3D printed using photosensitive resin. The proposed end-effector was assembled using a bolt that tightened the gripper and the connector. Of note, the swab is a thin and long rod which is relatively easy to be bulked when subjected to vertical force. Meanwhile, lateral force can also cause the bending of the swab stick. Both the above can potentially cause discomforts of the patient, which are to be monitored by the proposed design, i.e. the excessive vertical force due to the buckling effect and the force or torque in the lateral direction.

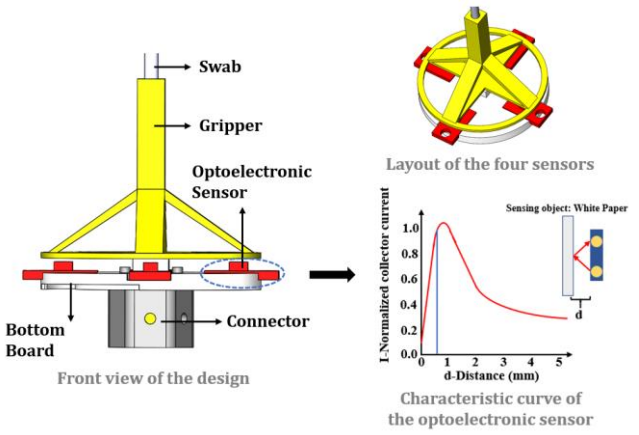

Fig. 3. Schematic illustration of the end-effector design based on a force-sensing gripper with embedded optoelectronic sensors.

III. Finite Element Analysis

A. Passive Compliant Mechanisms

Finite Element Analysis (FEA) was used to investigate the design of the passive compliant mechanisms, using the software Abaqus (ver. 2016). The material of the swab stick is ABS, with a Young's modulus of 1600 MPa and a Poisson's ratio of 0.394. The material of the 3D printed fixture has a Young's modulus of 2600 MPa and a Poisson's ratio of 0.43. The Young's modulus and the Poisson's ratio were obtained from the 3D printing service company. The interaction between the soft structure and the fixture is tie and so is the interaction between the fixture and the swab. The analysis was performed with 0.01 N and 0.02 N lateral force applied to the tip of the swab to different design configurations. As the design aims to adaptively adjust the posture of the swab in a sensitive way, small forces were tested for the FEA and the following bench experiment. The displacement of the swab tip is displayed in Table I and a deformation example is shown in Fig. 4. It can be seen that with the same amount of force exerted on the tip of the swab, the swabbing system with the compliant mechanism has increased flexibility.

TABLE I. Displacements of the Swab for Different Configurations

Lateral force	No compliant mechanism	Config I	Config II	Config III
0.01 N	3 mm	27 mm	7 mm	20 mm
0.02 N	6 mm	53 mm	14 mm	39 mm

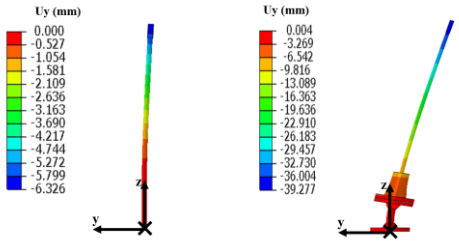

Fig. 4. FEA of the swabbing system with 0.02 N exerted laterally on the side of the swab without and with the passive compliance mechanism.

B. Active Force-sensing Gripper

Based on the data from experiments [5, 7], the lateral loading varying from 0-0.4 N with interval of 0.1 N was used for the FEA analysis. The axial force that would cause buckling of swab was set at 2.5 N based on the practical test. The ABS used to 3D print the gripper has the Young's modulus of 1600 MPa and Poisson's ratio of 0.43. In this analysis, thickness of the gripper's deflection beam that influences the detecting range of force was also investigated, including the setting of 0.8 mm, 1.0 mm, 1.2 mm, and 1.5 mm. For the vertical force test, an example of the gripper's displacement in Z direction under 2.5 N is shown in Fig. 5(a). For the lateral force test, an example of gripper's deformation at the top of optoelectronic sensor when subjected to 0.3 N is shown in Fig. 5(b). The influence of the gripper's thickness on the resulting displacement of the gripper under 2.5 N vertical load is shown in Fig. 5(c), where the maximum deflection is 0.55 mm for the thickness of 0.8 mm, and the minimum is 0.15 mm for the thickness of 1.5 mm. The relationships of the displacement and the applied lateral force for different thickness settings are shown in Fig. 5(d).

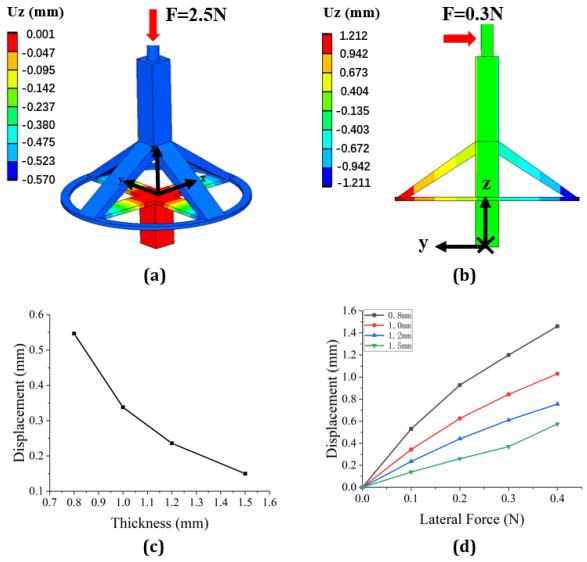

Fig. 5. FEA results that show: (a) displacement for 0.8 mm-thickness gripper under 2.5 N vertical force, (b) displacement for 0.8 mm-thickness gripper under 0.3 N lateral force; (c) displacement under axial loading of 2.5 N for gripper with different thickness; and (d) displacement under lateral loading from 0-0.4 N for gripper with different thickness.

IV. Experiments and Results

A. Passive Compliant Mechanism

Experiments were performed to validate the results from the FEA. The swab used in this experiment is a standard NP swab (total length of 150 mm) attached to the fixture. Forces were exerted to the swab by hanging a weight of 1 g, 2 g at the tip of the swab, as indicated in Fig. 6 (a) and (b). A ruler was placed vertically to record the positions and the lateral displacement was calculated by the position of the swab with the weight hanging at the tip minus the position of the swab without the weight hanging at its tip. The experiment was performed first by attaching the swab to the fixture with the fixture fixed to the clamp (Fig. 6(a)), then with the fixture connected to the compliant mechanisms and the connector fixed to the clamp (Fig. 6(b)). The results of the experiment are displayed in Table II. It can be seen that the use of the passive compliant mechanisms would increase the flexibility of the swabbing system. Different configurations would result in different bending stiffnesses, as indicated by the lateral displacements. To test the impacts of the compliant mechanism on the vertical direction, a force sensor (JHBM-H3, JNSensor, Anhui, China) was fixed to a moving platform along with a digital caliper attached to measure the displacement. By pressing the tip of the swab until the buckling effect occurs, the critical forces and the corresponding displacements were recorded (Table III). It can be observed that the use of the passive compliant mechanisms would effectively reduce the critical force, preventing excessive force exerted on patients.

TABLE II. Displacements of the Swab for Different Configurations

Lateral force	*No compliant mechanism*	*Config I*	*Config II*	*Config III*
0.01 N	3 mm	33 mm	10 mm	20 mm
0.02 N	6 mm	59 mm	17 mm	37 mm

TABLE III. Critical Forces and Displacements of the Swab Due to the Buckling Effect When Subjected to Vertical Load

	No compliant mechanism	*Config I*	*Config II*	*Config III*
Critical force/N	2.50	0.90	1.00	1.10
Displacement/mm	20.60	16.10	25.60	10.60

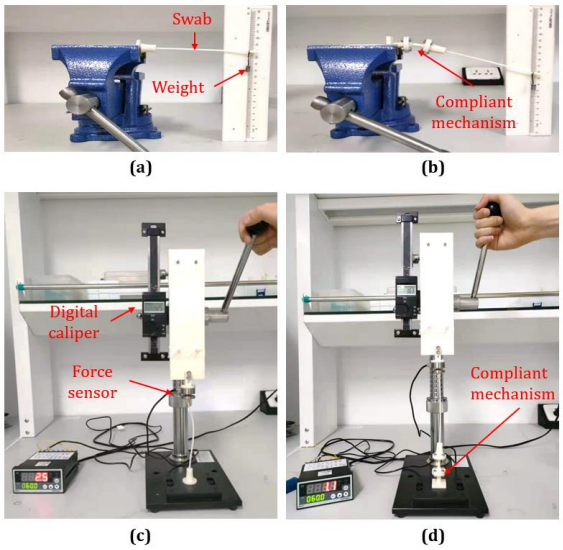

Fig. 6. Experimental setups to test: (a) lateral force exerted on the swabbing system, (b) lateral force exerted on the swabbing system with the compliant mechanism attached, (c) vertical forces applied to the swab, and (d) vertical forces applied to the swab with the compliant mechanism attached.

B. Active Force-sensing Gripper

The force-sensing gripper was calibrated by applying different weights in lateral direction. With the gripper firmly clamped, different torques were exerted by hanging weights at different locations on the swab stick (Fig. 7(a)). The output voltage signals were recorded with slowly generated torques (Fig. 8) using a single-board microcontroller (Arduino Uno, 5 V, 10-bit ADC). The initial gap between optoelectronic sensor and gripper was set at 0.8 mm to meet the first linear detecting range, as indicated in Fig. 3. The gripper with 0.8 mm, 1.0 mm, 1.2 mm, and 1.5 mm thickness was tested in the experiments, respectively.

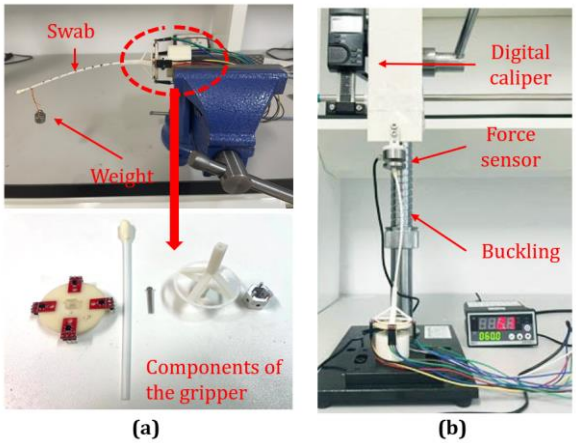

Fig. 7. Experimental setups to test: (a) lateral force applied to the force-sensing gripper and (b) buckling effect under critical force.

As can be seen in Fig. 8, the linearity could be obtained under certain torque range and the sensitivity is increased with the thickness of gripper deceasing. A line fitting was applied to capture the relationship between torque (T) and voltage (V). The effective measurement ranges of the force for gripper with different thickness are shown in Table IV. It is observed that by adjusting the thickness of the gripper, different measurement requirements could be achieved. For buckling effect, the force-sensing gripper with a bonded swab was fixed onto the test rig. The vertical force, measured by the commercial force sensor, was applied to the tip of the swab slowly until the obvious buckling effect is observed (Fig. 7(b))). The output voltage signals of the grippers with different thicknesses and the applied forces were recorded (Table V). The buckling effect can be detected up to 2.5 N.

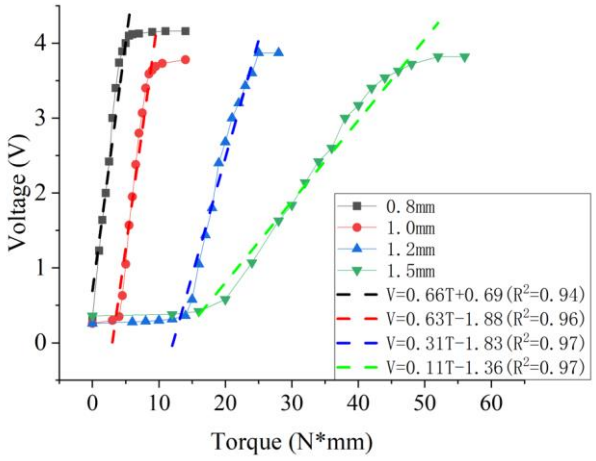

Fig. 8. Relationship between the applied torque and the output voltage measured by the optoelectronic sensor for grippers with different thicknesses.

TABLE IV. MEASURABLE FORCE RANGES FOR THE SENSING GRIPPERS WITH DIFFERENT THICKNESSES

	Sensing grippers with different thicknesses			
	0.8 mm	***1.0 mm***	***1.2 mm***	***1.5 mm***
Force Range (N)	0-0.03	0.04-0.07	0.12-0.20	0.16-0.35

TABLE V. RRESULTS OF THE BUCKLING EXPERIEMENTS

	Sensing grippers with different thicknesses			
	0.8 mm	***1.0 mm***	***1.2 mm***	***1.5 mm***
Critical Force (N)	1.50	2.00	2.00	2.50
Voltage (V)	4.11	4.13	3.57	2.50

V. CONCLUSION

In this study, we proposed two novel end-effector designs that can be equipped at the distal end of a robot to passively regulate or actively sense the forces exerted on the patients during the robot-assisted NP or OP swab collection procedure. Both the end-effectors are detachable, recyclable, cost-efficient, and can work with a variety of existing robot configurations used to combat respiratory infectious diseases, e.g. serial, parallel, or continuum. The two end-effector designs have been analyzed by FEA and experimentally validated with bench tests.

The first design relies on compliant mechanisms and utilizes flexible materials. It is concluded that the use of the proposed mechanisms can increase the flexibility of the swabbing system when subjected to lateral force, adaptively adjust the posture of the swab through body deformation, and therefore avoid excessive force. By changing the configuration of the mechanism, different bending stiffness can be obtained. The use of the mechanisms can also effectively reduce the critical force in the vertical direction when the buckling effect occurs. The second design relies on active sensing of the force or torque based on the deformation of the structure and the use of the optoelectronic sensors. It is concluded that the lateral force range that the force-sensing gripper can detect is 0-0.35 N depending on the different thickness of the gripper and the vertical force range causing buckling effect that can be sensed by gripper is 1.5-2.5 N. Additionally, by combining use of the four optoelectronic sensors, the direction of the force can also be predicted.

In the future, we will focus on integrating the proposed two end-effector designs into the off-the-shelf robots to test their functionalities in more realistic scenarios. The material and structural configuration for the passive compliant mechanism will be optimized to achieve appropriate level of compliance to meet the clinical needs and the proposed force-sensing gripper will be manufactured with improved processing technology mechanically and electronically.

REFERENCES

[1] A. Gao *et al*., "Progress in robotics for combating infectious diseases," *Sci. Robot*., vol. 6, no. 52, 2021.

[2] P. Courtney and P. G. Royall, "Using Robotics in Laboratories During the COVID-19 Outbreak: A Review," *IEEE Robot. Autom. Mag.,* vol. 28, no. 1, pp. 28-39, 2021.

[3] Y. Shen *et al*., "Robots Under COVID-19 Pandemic: A Comprehensive Survey," *IEEE Access*, vol. 9, pp. 1590-1615, 2021.

[4] S. Wang, K. Wang, R. Tang, J. Qiao, H. Liu and Z. -G. Hou, "Design of a Low-Cost Miniature Robot to Assist the COVID-19 Nasopharyngeal Swab Sampling," *IEEE Trans. Med. Robot. Bionics*, vol. 3, no. 1, pp. 289-293, 2021.

[5] S. -Q. Li *et al*., "Clinical application of an intelligent oropharyngeal swab robot: implication for the COVID-19 pandemic," *Eur. Respir. J.*, vol. 56, no, 2, 2020.

[6] Y. Hu *et al*., "Design and Control of a Highly Redundant Rigid-Flexible Coupling Robot to Assist the COVID-19 Oropharyngeal-Swab Sampling," *IEEE Robot. Autom. Lett.*, 2021.

[7] Z. Xie *et al*., "A Tapered Soft Robotic Oropharyngeal Swab for Throat Testing: A New Way to Collect Sputa Samples," *IEEE Robot. Autom. Mag.,* vol. 28, no. 1, pp. 90-100, 2021 .

[8] S. Crowe, *Danish startup develops throat swabbing robot for covid-19 testing*, The Robot Report, May. 27, 2020. Accessed on: April. 30, 2021. Available:https://www.therobotreport.com/danish-startup-develops-throat-swabbing-robot-for-covid-19-testing/.

[9] Y. -L. Chen, F. -J. Song and Y. -J. Gong, "Remote Human-robot Collaborative Impedance Control Strategy of Pharyngeal Swab Sampling Robot," in *Proc. 2020 IEEE Int. Conf. Autom. Control Robot. Eng.*, pp. 341-345.